GEOLOGICA CARPATHICA, 51, 1, BRATISLAVA, FEBRUARY 2000
49–57

DISSOLUTION OF K-FELDSPAR INTO Si-Al GEL AND CRYSTALLIZATION OF HALLOYSITE IDENTIFIED IN THE KAOLIN DEPOSIT OF SÃO VICENTE DE PEREIRA (PORTUGAL)

IULIU BOBOS and CELSO GOMES

Department of Geosciences, University of Aveiro, Aveiro-3810, Portugal

(Manuscript received January 18, 1999; accepted in revised form September 28, 1999)

Abstract: Dissolution of K-feldspar into Si-Al non-crystalline phase was identified in the kaolin deposit of São Vicente de Pereira (Portugal). The gel having a SiO_2/Al_2O_3 ratio approximately equal to the unity, crystallized into halloysite-0.7 nm. SEM investigations carried out on K-feldspar grains show a vacuolar texture characterized by etch-pits of various dimensions. The pits exhibit various shapes, either polygonal or circular. The gel was identified by SEM on the K-feldspar surfaces and by TEM in the < 2 μm clay fractions. TEM images display tubes of halloysite-0.7 nm surrounding flakes of Si-Al gel. Relicts of K-feldspar pseudomorphs submitted to amorphization are identified by TEM. SAED analyses confirmed the non-crystalline state of the gel. Electron microprobe analyses attested a very fast destabilization of the chemical structure of K-feldspar grains.

Key words: Portugal, kaolin deposit, scanning and transmission electron microscopy, X-ray diffraction, K-feldspar dissolution, Si-Al gel, halloysite-0.7 nm.

Introduction

Alteration of feldspars into kaolinite is due to weathering or hydrothermal processes (e.g. Keller 1978; Wilke et al. 1978; Meunier & Velde 1979; Anand et al. 1985, among others). The nature of feldspar alteration and formation of secondary minerals is strictly related to geochemical environments. Several cases of feldspar weathering have been well documented by high resolution-transmission electron microscopy investigations (Eggleton & Buseck 1980; Banfield & Eggleton 1990; Robertson & Eggleton 1991). These contributions concluded that feldspar alteration produce secondary phases either illite or dehydrated smectite via non-crystalline intermediate phases and then, kaolinite or halloysite is formed. Feldspar alteration can produce kaolinite directly from solution and halloysite via a non-crystalline phase (Eswaran & Bin 1978), whereas epitactic/topotactic alteration of K-feldspar into secondary minerals is not possible (Gilkes et al. 1986). Romero et al. (1992) have shown the transformation of feldspar into proto-crystalline material similar to allophane either in composition or morphology. Therefore, it is assumed that the feldspar alteration involves two distinctive processes: i) dissolution of feldspars into solution and ii) subsequent precipitation from solution of kaolinite or other mineral phases.

Non-crystalline Fe-Si-Al- oxy-hydroxides and amorphous aluminium hydroxide have been identified as being formed from feldspars at the earliest weathering stage (Eggleton 1987). Other papers reported that Fe and Si rich high defect fibrous materials are transformed into halloysite (Tazaki & Fyfe 1987). Sequences of gibbsite are always associated with weathering of feldspar. However, other authors (Berner & Holdren 1979) did not find surficial layers of secondary material on the weathered feldspars surfaces.

Feldspar dissolution kinetics is a subject thoroughly studied (e.g. Murphy & Helgeson 1987; Drever 1994; Blum & Lasaga 1991, etc.) and the majority of the publications suggest that feldspar dissolution rates are pH independent in the range ~ 5 to 8.

It is well known from literature that hydrated halloysite (i.e. halloysite-1 nm), is formed from glass rich volcanic materials and displays spherulitical or spheroidal morphology (Kirkman 1975, 1977, 1981; Gomes & Massa 1991) and halloysite-0.7 nm showing tubular morphology is formed from feldspars or micas (Estoule-Choux & Blanchet 1987). Synthesis experiments accomplished by Parham (1969) in the laboratory supported the idea that halloysite-0.7 nm represented an early stage of structural organization in the process of kaolin formation.

In the present paper K-feldspar grains collected in the kaolin deposit of São Vicente de Pereira (Portugal), were chemically and morphologically studied by electron microscopy techniques, in order to identify a relationship between K-feldspar and halloysite-0.7 nm, the ultimate product of alteration.

Geological background

The kaolin deposit of São Vicente de Pereira is situated at the north-western border of the Ossa Morena zone (Fig. 1) and it is widely extended along an alignment NNW-SSE, parallel to the fault which separates the Lourosa Unit from the Arada Unit. The estimated kaolin deposit extension is

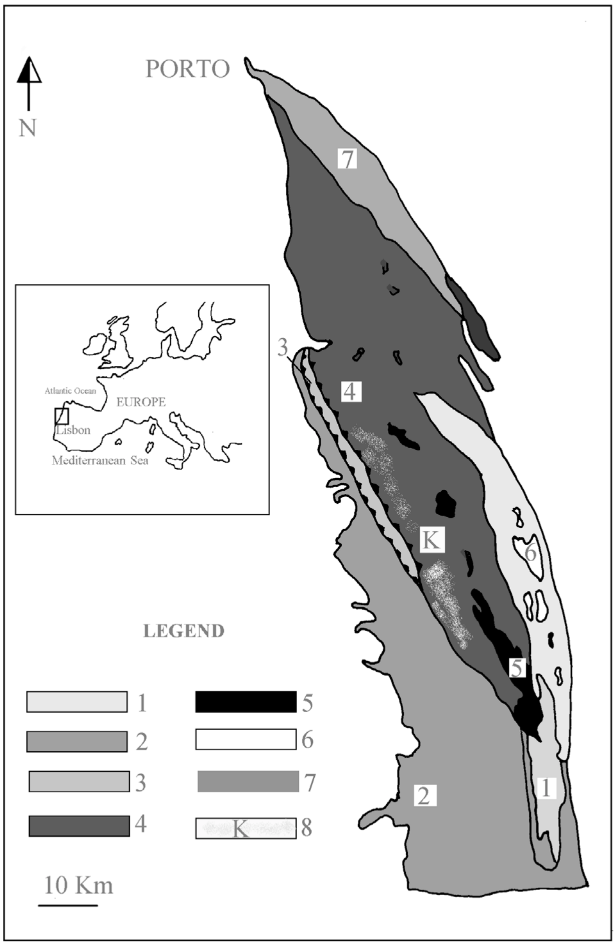

Fig. 1. Geological sketch of the northwestern sector of Ossa Morena zone (after Chaminé et al. 1995). 1: São João de Ver Unit (metavolcanite; metaporphyry; micaceous schist; metagraywacke); 2: Arada Unit (green schist; amphibolite schist; amphibolite; black quartzite); Espinho Unit (staurolite + micaceous schist; quartzite with garnet) Lourosa Unit (micaceous schist; ortho-gneiss; migmatite; amohibolite); 5: Hercynic Granitoids (syn D3); 6: Ante-Hercynic Granitoids; 7: Post-tectonic (Granitoid of Madalena); 8: Deposit of Kaolin (K), argillic alteration zone.

approximately 11 km^2. The Lourosa Unit, is characterized by HP metamorphism (sillimanite, garnet, K-feldspar) and includes several injection dykes of a two mica granitoids. The kaolin deposit of São Vicente de Pereira is related solely to migmatite rocks exhibiting argillic alteration. The textural integrity of migmatite rocks is well preserved in several places of São Vicente de Pereira kaolin deposit, being recognized several facies, such as: equigranular, fine-grained, granophyric and pegmatite. Hydrothermal activity in the kaolin deposit of São Vicente de Pereira and to the north of the deposit, is associated with a deformational system which includes faults, fractures and dilatation zone — ductile shear zone — (Bobos & Gomes 1998). Hydrothermal fluids were genetically and spatially related to fluids of metamorphic origin and felsic intrusive rocks (Bobos & Gomes, unpublished data).

Two types of alteration stages were described: hydrothermal and supergene (Bobos & Gomes 1998). Hydrothermal alteration is characterized by a relict greisen type alteration, represented by quartz + muscovite bearing F, Cl and quartz + tourmaline assemblages, and by an argillic alteration represented by well ordered kaolinite. Silicification and tourmalinization are two late hydrothermal processes identified in the São Vicente de Pereira area, as well as in the north part of this area. The quartz ± tourmaline bearing assemblage occurs as veins of 10 to 15 cm wide and veinlets of disseminated tourmaline in the argillized zone.

Weathering is expressed by poorly ordered kaolinite ± illite assemblage, as well as by kaolinite into halloysite-0.7 nm transformation (Tari et al. 1999; Bobos & Gomes, unpublished data). Two generations of halloysite-0.7 nm were distinguished by TEM: one formed from kaolinite and the other from K-feldspar; the last being the aim of the present paper.

In the kaolin deposit of São Vicente de Pereira, fenocrystals of K-feldspar are completely altered into halloysite-0.7 nm, sometimes associated with poorly ordered kaolinite. Small K-feldspar grains silicified and undigested by hydrothermal solutions, were found inside of the deposit; they were submitted to morphological investigations. Usually, they occur in a relict pegmatite facies. For comparison apparently fresh K-feldspar grains occurring in the unaltered migmatite complex, were morphologically investigated as well.

Materials and methods

Separation of the < 2 μm fractions in the alteration products of K-feldspar grains and kaolin rock were carried out by the sedimentation method using Stoke's law. Dispersion of clay minerals has been achieved without any chemical treatment, except the use of ammonia buffer in the suspension (three drops of ammonia for one litre of distilled water). All the separated clay fractions were washed up and concentrated by centrifugation. The < 2 μm clay fractions were air-dried at 40 °C overnight to avoid a possible conversion of halloysite-1 nm into halloysite-0.7 nm. The amorphous phase was extracted from K-feldspar grains collected inside the kaolin deposit, using Jackson's (1974) technique (chapter II, pp. 72) and then, XRD analysed.

Samples of K-feldspars, as well as specimens containing the < 2 μm clay fractions of their alteration products, prepared as non-oriented mounts were examined by X-ray diffraction (XRD) with a Rigaku Geigerflex D/max. — C series machine, using Cu$K\alpha$ radiation and a scanning speed of 1° 2θ, per min.

The sample of halloysite-0.7 nm have been previously described from the structural and morphological points of view (Bobos et al. 1996), being investigated again in order to check a relationship between gel and halloysite-0.7 nm.

Morphological investigation was carried out using a scanning electron microscope (Jeol JSM-35C), equipped with EDAX facilities and operated at an accelerating voltage of 15 kV. A few partially altered K-feldspar grains were crushed into several small grains and then cleaned ultrasonically. Samples of these remaining grains were mounted on a carbon holder and then, gold coated.

Microscopic observation was carried out with a Hitachi H-9000 transmission electron microscope (TEM), working at

80 kV, equipped with an X-ray energy dispersive spectrometer (EDAX) and selected area electron diffraction (SAED). SAED was used to determine the crystalline or amorphous character of the secondary phases, using apertures of 5–50 µm, in order to select 1–1.5 μm^2 areas of the mineral. For calibration of the SAED patterns an internal standard of gold was used. The < 2 µm fractions were dispersed using an ultrasonic bath and from the dispersion, after a convenient dilution, a few drops of the suspension were spread over copper microgrids. All microgrids were covered with a Formvar film, used as a specimen holder.

Results

X-ray diffraction

K-feldspar grains and the < 2 µm clay fractions were investigated by XRD, in order to appreciate both structural characteristics and degree of alteration.

XRD traces of K-feldspar grains, show well resolved d_{hkl} reflection lines (Fig. 2a and b). The two XRD patterns of K-feldspar show differences in intensity of both the 131 and 1**3**1 reflection lines. Also, the intensity decreases for both the **24**1 and **2**41 reflection lines. This means, that some order–disorder structural transformation took place in the K-feldspar structure.

The height of the background of XRD patterns of K-feldspar grains increases in the range of 20–40 (° 2θ), which means that an amorphous phase is its associated. Quartz and small amounts of illite (< 3 %) were found associated with K-feldspar.

Aluminosilicate gel extracted from K-feldspar grains was XRD recorded. The XRD pattern obtained, exhibits a general linear background, except for a broad diffusion peak in the range of 20–35, (°2θ).

The XRD pattern of halloysite-0.7 nm (Fig. 2c) is characterized by the increase of the (020) reflection line intensity, whereas the (1**1**0) and (11**1**) reflection lines appear just as weak modulations of the (02,11) diffraction bands. Besides, the (001) reflection line has an asymmetrical shape. The halloysite-0.7 nm sample is not admixed with kaolinite as revealed after hydrazine treatment (Range et al. 1969).

The sample shown in Fig. 2c was selected from a well ordered kaolinite to halloysite-0.7 nm transition series identified in the same geological profile of the kaolin deposit (Bobos et al. 1996).

Electron microscopy

SEM

K-feldspar grains were collected from two distinct places: outside and inside the kaolin deposit. The surfaces of the K-feldspar grains were examined. The typical cleavage planes are still preserved (Fig. 3a) in K-feldspar megacrystals, that had been collected in the unaltered migmatite complex. Weathering products, having irregular forms, are identified in the right side of the same picture (Fig. 3a). Electron microprobe analyses indicated for those weathering products high contents of Al and small contents of Si, Fe and K.

Altered K-feldspar grains, collected inside the kaolin deposit, exhibit "porous" surfaces. On the other hand, at the surfaces of altered K-feldspar grains, belonging to the pegmatite facies, both structural and morphological changes could be observed; the last is characterized by vacuolar structure exhibiting etch-pits of variable dimensions (Fig. 3b). As a rule, the pits are well aligned along the K-feldspar crystal cleavage planes. However, an ordered alignment of the pits couldn't be identified. In fact, a disordered network of pits was identified (Fig. 3c and 3d). The pits exhibit various shapes from rhombic to large polygonal holes. They indicate, that the K-feldspar has been rapidly dissolved or "corroded" by solutions with an acid pH, whereas no secondary mineral phases were produced. Also, no intermediate mineral phases were recognized on K-feldspar surfaces by SEM. Small amorphous flakes, 2–3 µm in size, with a Si-Al composition on the K-feldspar surfaces could be identified. The flakes exhibited a light white colour and are concentrated in a small nucleus (Fig. 3c and 3d). The flakes of Si-Al gel growth on K-feldspar grains were identified, even after thoroughly cleaning grains with ultrasound. Probably, they correspond to epitaxial growths on feldspar grain surfaces. Various zones showing either agglomerated or isolated flakes of Si-Al composition were also identified (Fig. 3c and 3d). From these flakes, small tubular crystals of halloysite-0.7 nm were nucleated and then, grown in sheaf-like agglomerates. Several sheaves of halloysite-0.7 nm tubes were also identified in large holes on K-feldspar surfaces. Detailed images of halloysite-0.7 nm tubes grown in sheaf-like agglomerate are shown in Fig. 3e and 3f. However, isolated tubes of halloysite-0.7 nm and very small pseudohexagonal kaolinite plates (< 0.5 µm) can be clearly observed in the pictures (Fig. 3b and 3f).

TEM

The < 2 µm clay fractions extracted from the altered K-feldspars and the < 2 µm halloysite-0.7 nm fractions (Fig. 2c) were investigated by TEM. The sample whose XRD pattern is shown in Fig. 2c, contains both long and short tubes of halloysite-0.7 nm, Si-Al gel and partially rolled kaolinite plates. Rolled kaolinite plates do not constitute a subject of the research being carried out.

Non-crystalline irregular plates with $SiO_2/Al_2O_3 \approx 1$ (resulting from analytic electron microscopy) were identified in the < 2 µm fractions extracted from the K-feldspar. The Si-Al gel was derived from the dissolution of K-feldspar. Relict pseudomorphs or amorphized feldspar crystals, recognized by their habit, are observed in the < 2 µm clay fractions (Fig. 4a). An incipient rolling-up at flake edges of Si-Al gel or a "crinkle" film was recognized. Small halloysite-0.7 nm tubes surrounding the irregular flakes of Si-Al gel (Fig. 4b and 4c) could be identified. Large and small folding could be identified seen. In Fig. 4c is shown the gel and the tubes of halloysite-0.7 nm, whose XRD pattern is shown in

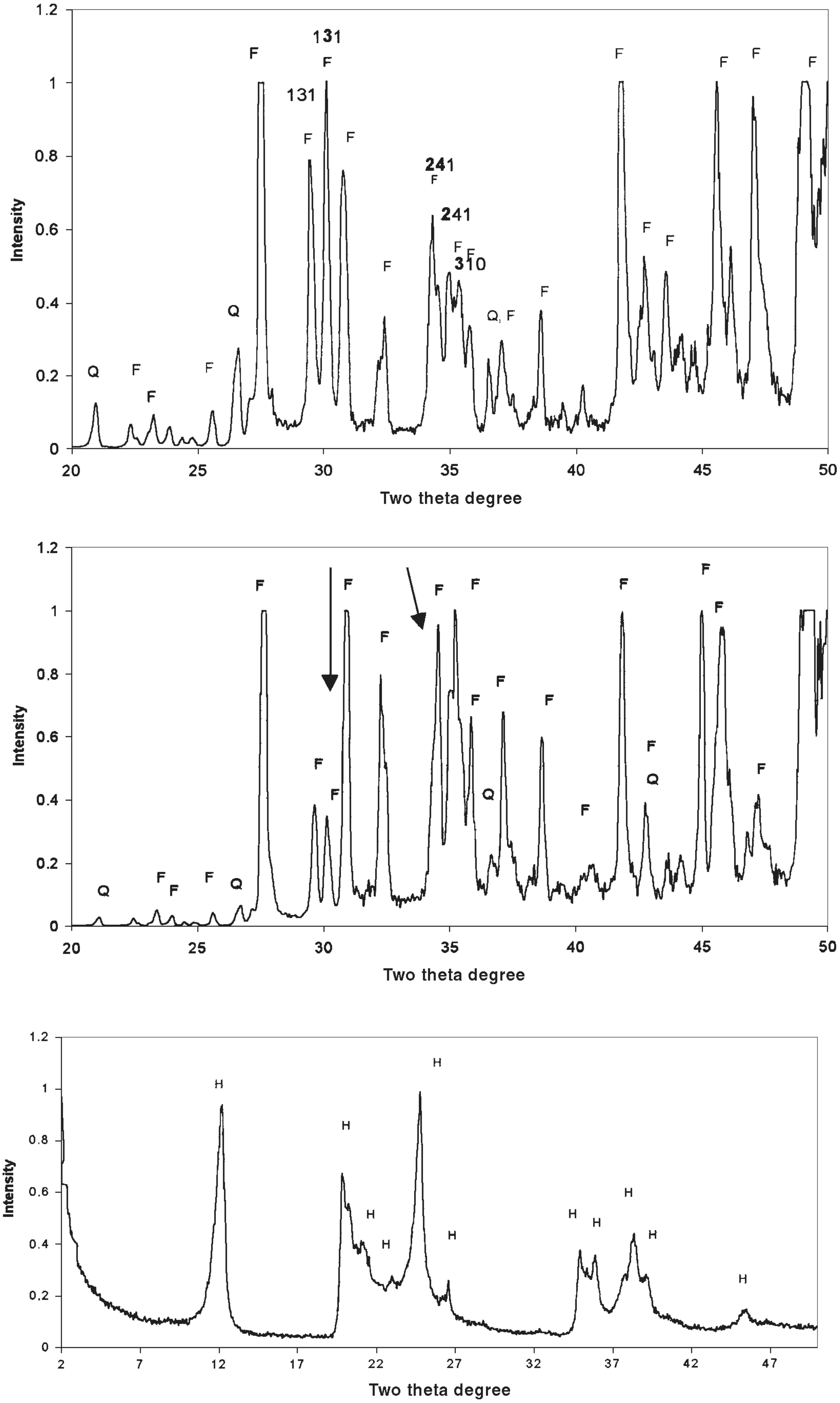

Fig. 2. XRD patterns (random specimens) of K-feldspars (a and b) and oriented specimens of halloysite-0.7 nm (c).

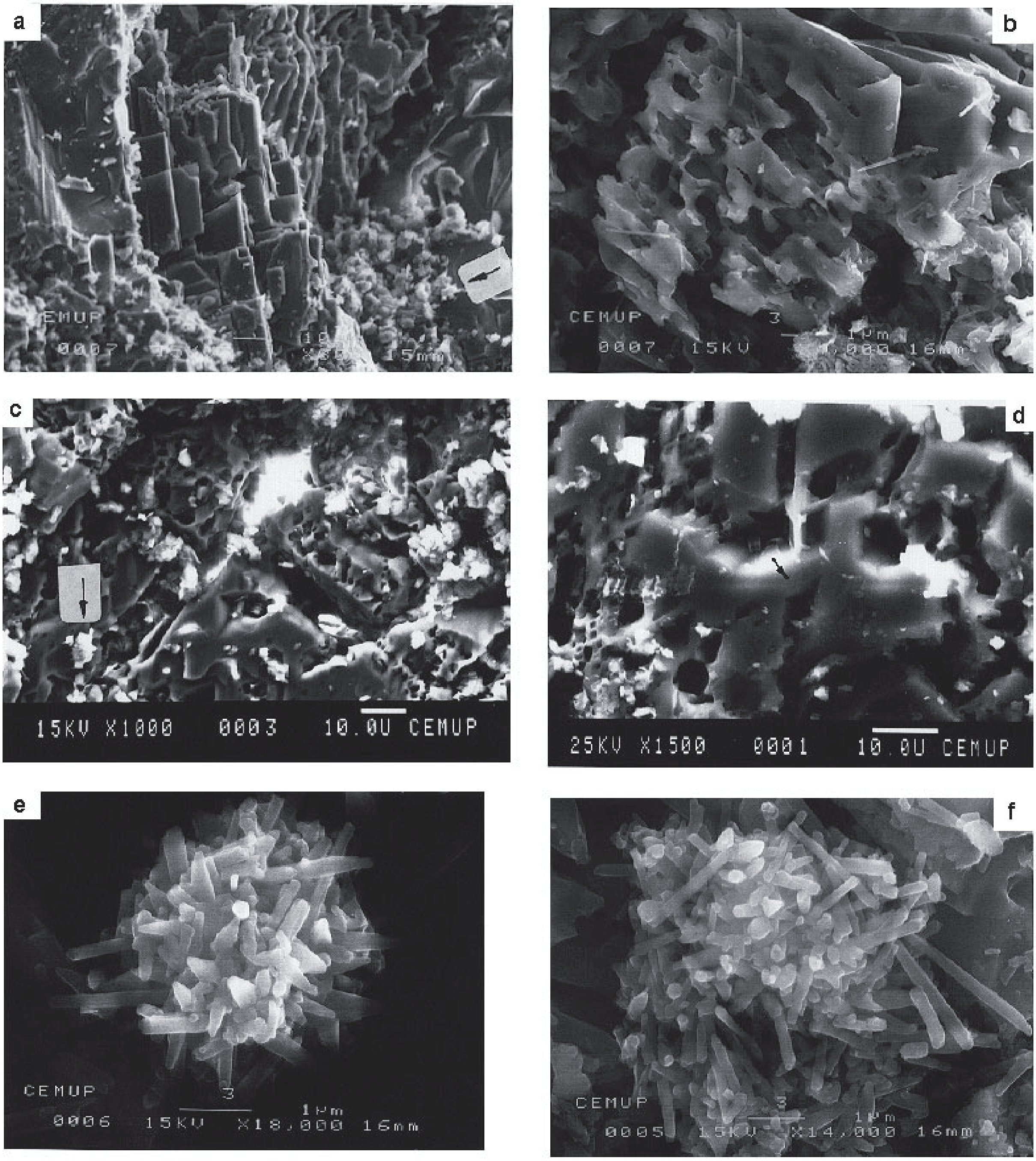

Fig. 3. SEM pictures of K-feldspar crystals and of agglomerates of weathering product characterized by high Al content and low Fe, Si and K contents (a). Etch-pits having polygonal or circular shapes are observed on K-feldspar (c, d, e); some rhombic shape are individualized and interpreted as being developed on the intersection of cleavage planes (b and d). Various flakes of Si/Al gel are well observed on K-feldspar surface (c and d). Tubes of halloysite-0.7 nm grown and associated in sheaves (e and f).

Fig. 2c. SAED carried out in the central region of one of the Si-Al gel flakes show only two very diffuse reflections rings (Fig. 4d). Close to the edges of the Si-Al gel flakes, crystallinity becomes slightly better. It appears that the amorphous phase corresponds to a precursor stage in the structural organization of 1:1 layers.

Electron microprobe analyses and analytic electron microscopy

Electron microprobe analyses carried out on feldspar grains show particular features of their chemical compositions (Table 1). Destabilization of feldspar structure is found to be very fast

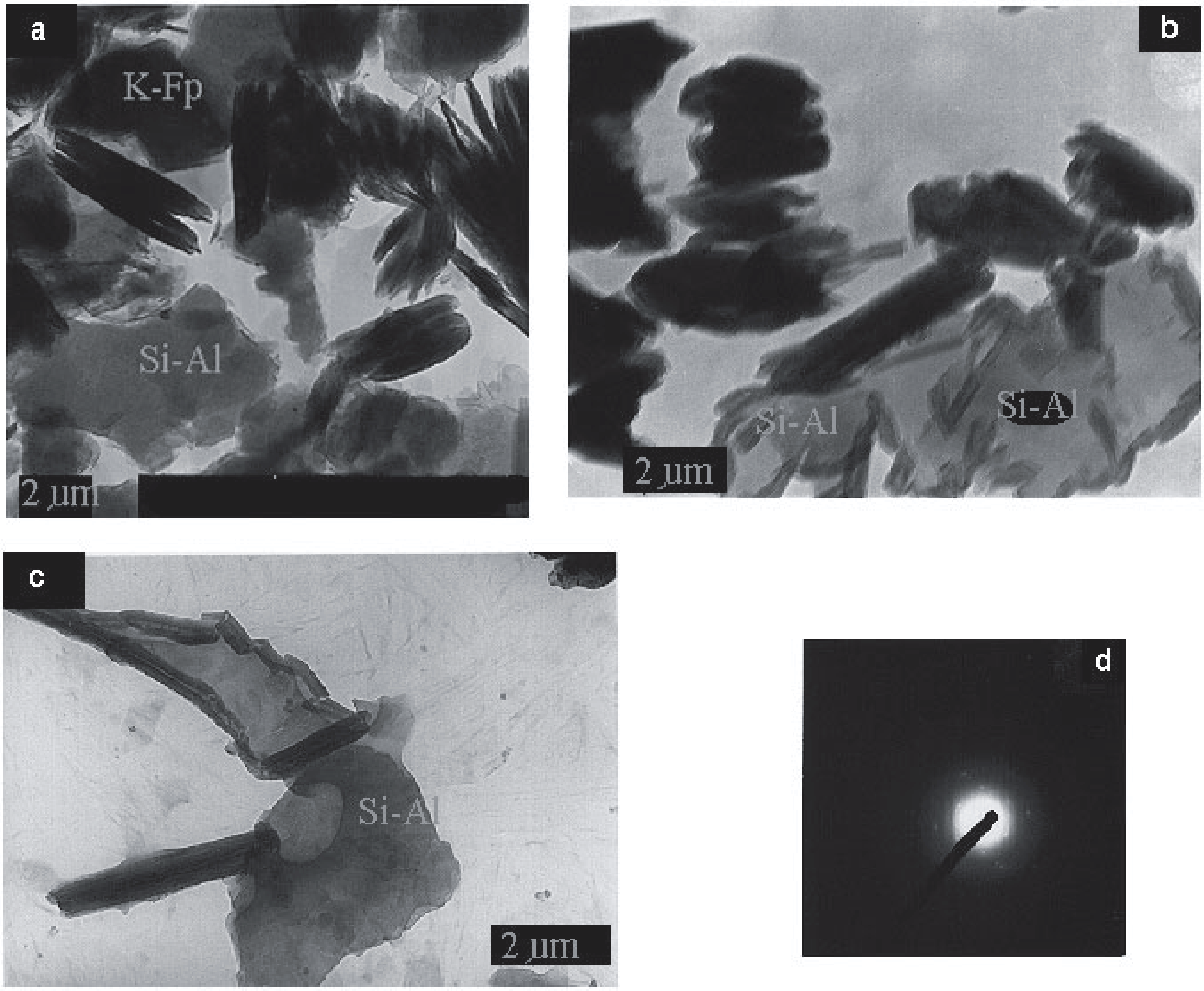

Fig. 4. TEM pictures of < 2 µm clay fractions showing K-feldspar pseudomorph submitted to amorphization and flakes of Si/Al gel (a). Tubes of halloysite-0.7 nm surround Si/Al gel flakes (b and d). SAED of Si/Al gel show an amorphous state (d).

Table 1: Electron microprobe analyses of K-feldspar and adjacent alteration product, and analytic electron microscopy of gel.

Samples	1 N = 3	2 N = 4	3 N = 4	4 N = 3	5 N = 8	6 N = 8	7 N = 4
SiO_2	62.94	62.35	60.70	64.07	56.4	56.14	50.36
Al_2O_3	17.52	18.35	21.84	19.37	37.89	39.36	49.74
FeO	0.01	0.44	0.58	0.67	2.07	2.11	0
CaO	0.13	0.27	0.03	0.11	0.13	0.08	0
MgO	0	0	0.05	0	0.24	0	0
Na_2O	0.92	0.88	0.15	1.05	0.05	0.08	0
K_2O	17.75	17.57	16.66	13.97	3.03	2.01	0
P_2O_5	0.50	0.24	0	0.47	0.18	0.13	0
SO_3	0.08	0	0	0.17	0	0	0
Cl	0.15	0	0	0.11	0	0	0
Total	100.00	100.00	100.00	100.00	100.00	100.00	100.00

(N = average chemical composition)
1, 2, 3: K-feldspar; 4, 5, 6: adjacent alteration product of K-feldspar; 7: Si/Al gel.

on a short scale (approximately equal to 5–10 µm), expressed by a loss of silica and alkaline elements and a gain of aluminium. Chemical changes took place from the edge of pits to the unaltered zone of K-feldspar crystal.

The presence of phosphorus and chlorine in the feldspar structure is assumed to be related to the chemistry of hydrothermal fluids (Bobos & Gomes, unpublished data).

In the ternary diagram (Fig. 5), the field corresponding to unaltered K-feldspar is noted with A. Chemical analysis related to altered K-feldspar are plotted in the field B, showing a loss of K and Si. Finally, the dissolution of K-feldspar passed to a gel having a SiO_2/Al_2O_3 ratio close to unity, whereas K is completely depleted. The silica resulting from the K-feldspar structure was removed in solution and then precipitated. Fe is not identified in the gel composition, being removed and then, incorporated probably into free iron oxide.

The flakes of gel recognized on the K-feldspar surfaces were found in the < 2 µm fractions and analysed by analytic electron microscopy. Their chemistry is simple, being composed solely of Si and Al.

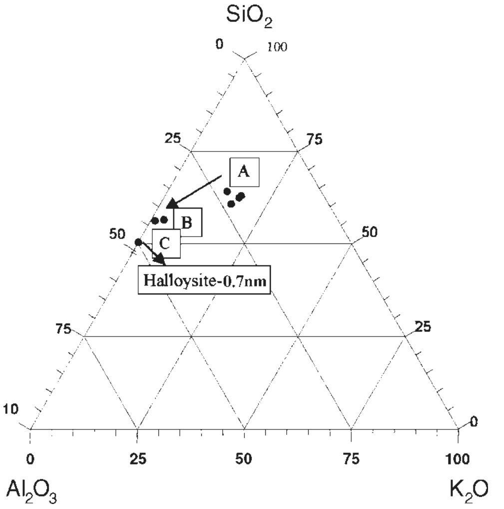

Fig. 5. Ternary diagram of SiO_2–Al_2O_3–K_2O. The quantitative chemical data of K-feldspar (Field A), alteration products (Field B), Si-Al gel phase (Field C) and halloysite-0.7 nm were plotted.

Discussion

The incongruent chemical reaction of the feldspar alteration (Hemley 1959) to common clay minerals, can be simply written:

$$KAlSi_3O_8 + 2H^+ + 9H_2O = Al_2Si_2O_5(OH)_4 + 4H_4SiO_{4(aq)} + 2K^+ \quad (1)$$
(K-feldspar) (Kaolinite)

Helgeson (1969, 1992) assumed that from the dissolution of feldspar, all its dissolved chemical constituents pass into the hydrolysing solution:

$$KAlSi_3O_8 + 4H^+ = K^+ + Al^{3+} + 3SiO_2 + 2H_2O \quad (2)$$
(K-feldspar) (Quartz)

$$KAlSi_3O_8 + 2H_2O = 3\,SiO_2 + K^+ + Al(OH)_4^- \quad (3)$$
(K-feldspar) (Quartz)

Theoretically, two different and independent chemical processes are involved in feldspar alteration. In particular, all the constituent elements of the K-feldspar are dissolved during H^+ activity and both reactions (2) and (3) can constitute a chemical path involved in the rapid dissolution of K-feldspar from São Vicente de Pereira kaolin deposit.

SEM investigations carried out on altered K-feldspar mineral grains show a vacuolar structure characterized by pits (polygonal holes) of variable dimensions. Partially altered K-feldspar grains exhibit "porous" surfaces, characterized by a dense and irregular network of pits of various sizes. This means that, K-feldspar has been dissolved or "corroded" by acidic solutions and then, transformed into Si-Al gel. No intermediate mineral phases were recognized by SEM on the K-feldspar surfaces, as we found on the K-feldspar surfaces collected outside the kaolin deposit. Various dislocations associated with strains in K-feldspar grains may contribute to the formation of reaction sites and to enhance the development of the etch pits. In an initial stage of the etch-pits, cross-section areas exhibiting rhombic shapes were developed apparently on the intersection of cleavage planes (Fig. 3a, 3b and 3c). The growth of hollow dislocations to form etch-pits and then enlargement of these pits, both associated with dissolution of K-feldspar, requires specific thermodynamic conditions and chemical affinity to the hydrothermal environment. Rapid dissolution of K-feldspar was the effect of the high circulation rate of ascending metamorphic waters and acid solutions along the north-western border of Ossa Morena zone, characterized by intense fracturing and shearing (Bobos & Gomes 1998).

In an acid environment the development of Al and Si-rich layers on the feldspar surface after dissolution, may provide favourable conditions for the crystallization of secondary phases such as clay minerals (Petrovic et al. 1976; Aagard & Helgeson 1983). It is also recognized that in acidic solutions, K-feldspar undergoes rapid and extensive exchange with H^+ forming a surface layer of hydrogen-feldspar several unit cells thick (Blum & Stillings 1995). In kinetic terms, several models of feldspar dissolution are described in the literature, where different parameters (e.g. pH, temperature, chemistry, stoichiometry, surface layer and charge density, etc.) are considered in the theoretical approaches and required by the feldspar dissolution process (Blum & Stillings 1995). Amorphous phases formed by precipitation from solution, are always thermodynamically unstable. However, the rapid dissolution of feldspar is poorly understood so far.

Two questions resulted from the material we investigated: what is the crystallization process of halloysite-0.7 nm from Si-Al gel? and why did form halloysite-0.7 nm from Si-Al gel and not kaolinite?

In natural waters, Al-aqueous species, depending on pH and temperature, both under temperate and tropical climate, were studied by Bourrie et al. (1989). The authors have shown a reaction scheme for Al precipitation related to pH, into monomeric species (e.g. Al^{3+} and $Al(OH)^{2+}$) at pH < 5 and then, into polymeric species at pH > 5, when gibbsite saturation is reached. Gibbsite and bohemite were not identified in our samples and it appears that halloysite-0.7 nm was formed without passing through intermediate mineral phases as described before.

According to Hem & Roberson (1967), dissolution of feldspar means a high tendency for hydrated Al to be tetrahedral co-ordinated by four hydroxyls. Merino et al. (1989) explained that Al in aqueous solutions is co-ordinated by six water dipoles and whenever pH increases some of the dipoles loose a hydrogen ion. Hydroxyl ions being produced, are attracted by the inner Al ion and co-ordinate hydroxyl ions around the Al, reducing the co-ordination number from 6 to 4. The pH of its environment is directly related to the negative charge of Si-Al gel. High pH values will favour Al tetra-co-ordination and low pH will favour Al hexa-co-ordination.

Nevertheless, the process seems to be more complicated. Several experimental studies of kaolinite synthesis from aluminosilicate gel are reported in the literature. Rodrigue et al. (1973) suggested that before kaolinite formation, the silica-alumina gel will form a structure composed of Si–O–Al–OH chains. De Kimpe et al. (1981) obtained kaolinite from aluminosilicate gels and confirmed the Si–O–Al–OH chains, as an intermediate stage in the formation of kaolinite structure. Besides, beyond the pH conditions, the authors have shown that the degree of hydrolysis of both gel and Si–O–Al–OH chains played a subsequent role in the process of kaolinite formation.

Thus, the incorporation of aluminium in tetrahedral sites of the structure can promote a strong tendency to curling (Bates 1959) and Al for Si substitution can cause bending of the 1:1 layers (Drever 1982). According to Merino et al. (1989) halloysite may crystallize when ^{VI}Al is dominant and ^{IV}Al is subordinate. However, the chemistry of the solution may control the morphology of crystals and therefore, the low or high supersaturated solution of Si and Al will favour the crystallization of kaolinite or halloysite-0.7 nm.

Analytical electron microscopy carried out on short and long tubes of halloysite-0.7 nm (Fig. 2c) shows that the Al:Si atomic ratio is greater than the unity (Tari et al. 1999), implying the presence of some tetrahedral co-ordinated Al. Neutron magnetic resonance spectroscopy (^{27}Al MAS-NMR) study carried out on halloysite-0.7 nm (Fig. 2c) identified a weak resonance at −70 ppm, ascribed to tetrahedral Al (Bobos & Gomes, unpublished data). Nevertheless, the analytical data is not yet available for the separated gel.

TEM shows thin and irregularly outlined of Si-Al gel plates. An increase of crystallinity towards the edges of these extremely thin plates is also clearly obvious by SAED as well as the presence of tubes of halloysite-0.7 nm developed on the edges. SEM observations carried out on K-feldspar surfaces identified halloysite-0.7 nm grown-up in sheaves, flakes of Si-Al gel, as well as separated tubes of halloysite-0.7 nm. Two nucleation processes of halloysite-0.7 nm are thought to have been developed: *i*) heterogeneous (individual halloysite-0.7 nm tubes in contact with K-feldspar surfaces) and *ii*) homogeneous (sheaves of halloysite-0.7 nm tubes formed of the bulk solution *via* Si-Al gel).

In the last process of halloysite-0.7 nm formation we assumed that the gel or quasi-gel is an intermediary or a proto-kaolinite structure composed of Si–O–Al–OH chains. The pH, temperature and chemistry of the solution played a main role in the organization of 1:1 immature layers. It appeared that a hydration process of both gel and 1:1 immature structure, is plausible for the explanation of halloysite- 0.7 nm formation from the Si-Al gel.

Conclusions

Weathering of feldspars should produce first smectite or illite and then, kaolinite. In other cases, early weathering of feldspar should produce some aluminium hydroxide, which is transformed into gibbsite, bayerite, nordstrandite, etc., depending on pH, temperature and electrolite concentration (Violante & Huang 1993).

In the kaolin deposit of São Vicente de Pereira the formation of halloysite-0.7 nm took place through a rapid dissolution of K-feldspar into Si-Al gel. No other minerals were identified. The structural organization of Si-Al gel would have passed through an intermediate stage, where the first Si–O–Al–OH chains were constituted. It seems that the greatest hydration took place in gel, before the formation of the first 1:1 immature layers.

Acknowledgements: I.B. thanks to Fundação para Ciȩncia e Technologia — Lisboa for the grant provided him (Praxis XXI BCC-4815). The authors are grateful to the three referees for the comments on the manuscript.

References

Aagard P. & Helgeson H.C. 1983: Activity/composition relations among aqueous solutions: II. Chemical and thermodynamic consequences of ideal mixing of atoms on homological sites in montmorillonites and illites, and mixed-layer clays. *Clays and Clay Miner.* 31, 207–216.

Anand R.R., Gilkes R.J., Armitrage T.M. & Hillyer J. 1985: Feldspar weathering in a lateritic saprolite. *Clays and Clay Miner.* 33, 31–43.

Banfield J.F. & Eggleton R.A. 1990: Analytical transmission electron microscope studies of plagioclase, muscovite and K-feldspar weathering. *Clays and Clay Miner.* 38, 77–89.

Bates T.F., 1959: Morphology and crystal chemistry of 1:1 layer lattice silicates. *Amer. Mineralogist* 44, 78–114.

Berner R.A. & Holdren G.R. jr. 1979: Mechanism of feldspar weathering. II. Observations of feldspar from soils. *Geochim. Cosmochim. Acta* 43, 1173–1186.

Blum A.E. & Lasaga A.C. 1991: The role of surface speciation in the dissolution of albite. *Geochim. Cosmochim. Acta* 55, 2193–2201.

Blum A.E. & Stillings L.I. 1995: Feldspar dissolution kinetics. In: White A.F. & Brantley S.L. (Eds.): *Chemical weathering rates of silicate minerals, Mineralogical Soc. Amer., Rev. in Mineralogy* 31, 291–355.

Bobos I., Gomes C. & Velho A. 1996: Kaolinite to halloysite-7Å transition in the kaolin deposit of São Vicente de Pereira (Portugal). In: Gomes C. (Ed.): *Proceedings of Eurolat'96, Rev. Univ. Aveiro, Geociȩncias* 10, 167–178.

Bobos I. & Gomes C. 1998: Greisen and post-greisen alteration in the kaolin deposit of São Vicente de Pereira (Portugal). *Canad. Mineralogist* 36, 1615–1624.

Bourrié G., Grimaldi C. & Régeard A. 1989: Monomeric versus mixed monomeric polymeric models for aqueous aluminium species: Constraints from low-temperature natural waters in equilibrium with gibbsite under temperate and tropical climate. *Chem. Geol.* 76, 403–417.

Chaminé H.I., Ribeiro A. & Pereira E. 1995: Cartografia geológica e estratigrafia da faixa precâmbrica do sector Espinho - Albergaria-A-Velha (Zona de Ossa-Morena). Faculdade de Ciȩncias, Univesidade do Porto, *Memória* 4, 329–333.

De Kimpe C.R., Kodama H. & Rivard R. 1981: Hydrothermal formation of kaolinite-like product from noncrystalline aluminosilicate gels. *Clays and Clay Miner.* 29, 446–450.

Drever J.L. 1982: The Geochemistry of natural waters. *Prentice-Hall,* Englewood Cliffs, NJ, 1–388.

Drever J.L. 1994: The effect of land plants on weathering rates of silicates minerals. *Geochim. Cosmochim. Acta* 58, 2325–2332.

Eggleton R.A. & Buseck P.R. 1980: High resolution electron microscopy on feldspar weathering. *Clays and Clay Miner.* 28, 173–178.

Eggleton R.A. 1987: Non-crystalline Fe-Si-Al-oxyhydroxides. *Clays and Clay Miner.* 35, 29–37.

Estoule-Choux J. & Blanchet C. 1987: L' alteration directe de muscovites et de biotites en halloysite: mise en evidence par microscopie electronique a balayage. *Clay Miner.* 22, 11–20.

Eswaran H. & Bin W.C. 1978: A study of deep weathering profile on granite in peninsular Malayesia: Mineralogy of the clay, silt and sand fractions. *Soil Sci. Soc. Amer. J.* 42, 149–158.

Gilkes R.J., Anand R.R. & Suddhiprakarn A. 1986: How to microfabric of soils may be influenced by the structure and chemical composition of parent minerals. *Trans. Int. Soil Sci. Conf. Hamburg* 6, 1093–1106.

Gomes C. & Massa M.E. 1992: Allophane and spherulitic halloysite, weathering products of trachitic pumice fall-outs in the Caldeira Velha area (S. Miguel-Azores). *Mineral. Petrogr. Acta* XXXV-A, 283–288.

Helgeson H.C. 1969: Thermodynamics of hydrothermal systems at elevated temperatures and pressures. *Amer. J. Sci.* 267, 729–805.

Helgeson H.C. 1992: Effects of complex formation in following fluids on the hydrothermal solubilities of minerals as a function of fluid pressure and temperature in the critical and supercritical regions of the systems H_2O. *Geochim. Cosmochim. Acta* 56, 3191–3207.

Hem D. & Roberson C.E. 1967: Form and stability of aluminium hydroxide complexes in dilute solution. *U.S. Geol. Survey, Water-Supply Pap.* 1827 A, 55.

Hemley J.J. 1959: Some mineralogical equilibrium in the system K_2O-Al_2O_3-SiO_2- H_2O. *Amer. J. Sci.* 257, 241–270.

Jackson M.L. 1975: Soil chemical analysis—advanced course. *Published by author,* Madison, Wisconsin, 1–895.

Keller W.D. 1978: Classification of kaolins exemplified by their textures in scanning electron micrographs. *Clays and Clay Miner*. 26, 1–20.

Kirkman J.H. 1975: Clay mineralogy of some tephra beds of Retorna area, North Island, New Zeeland. *Clay Miner*. 10, 437–449.

Kirkman J.H. 1977: Possible structure of halloysite disks and cylinders observed in some New Zeeland rhyolitic tephras. *Clay Miner*. 12, 199–216.

Kirkman J.H. 1981: Morphology and structure of halloysite in New Zeeland tephras. *Clays and Clay Miner.* 29, 1–9.

Merino E., Harvey C. & Murray H.H. 1989: Aqueous-chemical control of the tetrahedral-aluminium content of quartz, halloysite and other low-temperature silicates. *Clays and Clay Miner.* 37, 135–142.

Meunier A. & Velde B., 1979: Weathering mineral faces in altered granites:The importance of local small scale equilibrium. *Mineral. Mag.* 43**,** 261–268.

Murphy W.M. & Helgeson H.C. 1987: Thermodynamic and kinetic constraints on reaction rates among minerals and aqueous solutions. III. Activated complexes and the pH-dependence of rates of feldspar, pyroxene, wollastonite and olivine hydrolysis. *Geochim. Cosmochim. Acta* 51, 3137–3153.

Parham W.E. 1969: Halloysite rich tropical weathering products of Hong Kong: In: Heller L. & Weiss A. (Eds): *Proc. Int. Clay Conf. Tokyo,* 1, 403–416.

Petrovic R., Berner R.A & Goldhaber M.B. 1976: Rate control in dissolution of alkali feldspars. I. Study of residual grains by X-ray photoelectron spectroscopy. *Geochim. Cosmochim. Acta* 40, 537–548.

Range K.J., Range A. & Weiss A. 1969: Fire clay type kaolinite or fire clay minerals? Experimental classification of kaolinite–halloysite minerals. In: Heller L. & Weiss A. (Eds.): *Proc. Int. Clay Conf. Tokyo* 1, Israel Univ. Press, Jerusalem 3, 13.

Robertson I.D. & Eggleton R.A. 1991: Weathering of granitic muscovite to kaolinite and halloysite and plagioclase-derived kaolinite to halloysite. *Clays and Clay Miner.* 39, 113–126.

Rodrigue L., Poncelet G. & Herbillon A. 1972: Importance of the silica subtraction process during the hydrothermal kaolinization of amorphous silico-aluminas In: Seratosa J.M. (Ed.): *Proc. Int. Clay Conf. Madrid,*. Div. Ciencias C.S.I.C., Madrid, I, 187–198.

Romero R., Robert M., Elsass F. & Garcia C. 1992: Abundance of halloysite neoformation in soils developed from crystalline rocks. Contribution of transmission electron microscopy. *Clay Miner.* 27, 35–46.

Tari G., Bobos I., Gomes C. & Ferreira J.M. 1999: Modification of charge density during the kaolinite to halloysite-7Å transformation. *J. Coll. Interface. Sci.* 209, 360–366.

Tazaki K. & Fyfe W.S. 1987: Formation of primitive clay precursors on K-feldspar under extreme leaching conditions. In: Schultz L.G., Olphen van H. & Mumpton F.A. (Eds.): *Proc. Int. Clay Conf. Denver. Bloomington - Indiana,* 53–58.

Violante A. & Huang P.M. 1993: Formation mechanism of aluminium hydroxide polymorphism. *Clays and Clay Miner*. 41, 353–359.

Wilke B.S., Schwertman U. & Murad E., 1978: An occurrence of polymorphic halloysite in granite saprolite of the Bayerischer Wald, Germany. *Clay Miner.* 13, 67–77.